Manuscript submitted to: Volume 2, Issue 1, 16-27.

AIMS Materials Science DOI: 10.3934/matersci.2015.1.16

Received date 4 December 2014, Accepted date 17 March 2015, Published date 23 March 2015

Research article

Facile Synthesis and Structural Characterization of Co_3O_4 Nanocubes

Min Kang* and Hai Zhou

Department of Chemistry and Chemical Engineering, Zunyi Normal College, Zunyi 563002, PR China.

*** Correspondence:** Email: km20056570@163.com; Tel: +86-0851-28927159.

Abstract: Co_3O_4 nanocubes were synthesized via a simple hydrothermal method. X-ray diffraction (XRD) and high-resolution transmission electron microscopy (HRTEM) analysis revealed that the product was cubic single crystal Co_3O_4, with the width of several ten nanometers to several hundred nanometers. The influence of reaction temperature and the amount of dispersant on the size and morphology of the as-obtained Co_3O_4 were investigated. On the basis of condition-dependent experiments, a possible aggregate-dissolution-recrystallization growth mechanism was proposed to explain the formation process of the Co_3O_4 nanocubes. The catalytic activity characterization showed that the as-prepared Co_3O_4 nanocubes can catalyze the thermal decomposition of ammonium perchlorate (AP) effectively.

Keywords: hydrothermal; Co_3O_4; nanocubes; AP decomposition

1. Introduction

In recent years, great efforts have been invested in the crystallographic structure control over inorganic crystals, because of the unique electrical, optical, magnetic and catalytic characteristics compared to the corresponding bulk materials. The morphology of particles is closely related to the crystallographic surfaces enclosing the particles, and different crystal facets have different surface atom densities, electronic structure, bonding, and possible chemical reactivity. For example, γ-Fe_2O_3 nanorods enclosed by (110) and (100) facets showed excellent reactivity performance of selective catalytic reduction of NO with NH_3 [1], and TiO_2 enclosed by (011) facets exhibited higher light degradation ability than TiO_2 enclosed by (001) planes [2]. So, it is of great significance to synthesize crystals with the exposure of special facets.

Spinel cobalt oxide (Co_3O_4) possesses the normal spinel structure $A[B_2]O_4$, Co^{2+} ions occupies the tetrahedral (or *A*) sites and Co^{3+} ions occupies the octahedral (or *B*) sites [3]. The unit cell length of Co_3O_4 is 0.8084 nm and each cell comprises 56 ions [4]. Co_3O_4 has important technological

applications in many fields [5–8]. For example, Co_3O_4 is an important p-type semiconductor, and Co_3O_4 is also an important transition metal ceramic oxide, which has the potential of to be used in magnetism, sensors, electrochemical and catalysis [9–11].

In the last decade, several methods including solid-state reaction [12], thermal decomposition [9], microwave assisted synthesis [13], electrodeposition method [14], solvothermal/hydrothermal reaction with or without templates [15,16] and molten salt synthesis [17] were developed to prepare spinel cobalt oxide in nanoscale. So far, several Co_3O_4 nanocrystals with different morphology have been successfully synthesized, such as nanosheets [14], nanorods [17], flower-like structure [18], nanoboxes [19], nanobelts [20] and nanocubes [21,22]. Despite plenty of researchers reported their work about spinel cobalt oxide nanomaterials; however, most of the above-mentioned work focused on the final growth stage of Co_3O_4 and only a few reports investigated the growth process of Co_3O_4 [23,24]. As a result, it is meaningful to investigate the morphological growth process of Co_3O_4, which could provide some information about the crystal growth and design, and morphology-controlled synthesis of Co_3O_4 as well as some other inorganic building blocks.

Herein, we report a simple hydrothermal route to synthesize spinel cobalt oxide nanocubes using thiocyanate radical anions (SCN^-) as coordination ions. The influence of reaction parameters on the final morphology the Co_3O_4 nanocube was investigated, and a possible growth mechanism was proposed to explain the formation process of the Co_3O_4 nanocubes.

2. Experimental section

All the reagents were used without further purification: $Co(CH_3COO)_2{\cdot}4H_2O$ (99.5 wt%, analytical reagent (A. R.), Tianjin Fuchen Chemical Reagents Factory), NaSCN (98 wt%, A. R., Tianjin Tianda Chemicals Co., Ltd), poly(vinylpyrrolidone) (PVP, M_r = 50000, N content 12%–13%, A. R., Tianjin Guangfu Fine Chemical Research Institute). Double-distilled water was used throughout the experiment.

2.1. Synthesis of Co_3O_4 nanocubes

The typical synthesis process for Co_3O_4 nanocubes was as follows: 2 mM of NaSCN and 2 mM of $Co(CH_3COO)_2{\cdot}4H_2O$ were dissolved in 80 mL of distilled water under ultrasonic radiation, and then 0.003 mM PVP was added into the above mixture under ultrasonic radiation. The as-formed solution was sealed in a Teflon-lined autoclave of 150 mL capacity, and maintained at 120 °C for 36 h. After cooling to room temperature, the products were collected by centrifugation, and washed with distilled water three times and absolute ethanol twice to remove impurities. The final products were dried in air at 80 °C.

In order to investigate the growth process of the Co_3O_4 nanocubes, series of condition-dependent experiments were carried out. The reaction temperature was varied from 120 to 140, 160 and 180 °C to inspect the influence of reaction temperature. The mole ratio of PVP to Co^{2+} was altered from 0 to 0.002, 0.003 and 0.005 to investigate the influence of PVP. And the reaction time was altered from 2 to 9, 18, 27 and 36 h to observe the growth process of the nanocubes.

2.2. Characterizations

The products were characterized by transmission electron microscopy (JEOL JEM-1011 with an accelerating voltage of 80 kV), high-resolution TEM (JEM2010 at 200 kV accelerating voltage), scanning electron microscopy (XL30 S-FEG at 10 kV accelerating voltage), and powder X-ray diffraction (Rigaku D/max-rB diffractometer using Cu Kα radiation, λ = 0.15408 nm). The ammonium perchlorate decomposition activity of the samples was tested by thermalgravimetric analysis (TGA/SDTA851).

3. Results and Discussion

3.1. Phase and morphology of the Co_3O_4 nanocubes

Figure 1 shows the XRD pattern of the typically synthesized Co_3O_4 nanocubes. It can be seen that all peaks in the pattern can be perfectly indexed to cobalt tetroxide (JCPDS 42-1467) with cubic crystal system. The narrow sharp peaks suggest the high crystallization of the Co_3O_4 nanocubes. And no characteristic peaks of any other impurities are observed, indicating that pure cubic crystalline Co_3O_4 was obtained via the hydrothermal process.

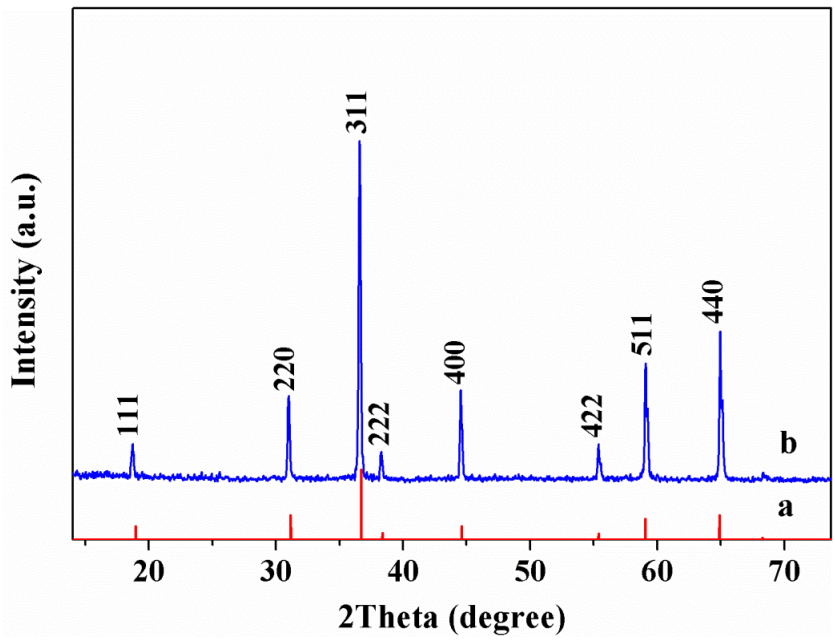

Figure 1. XRD patterns of (a) JCPDS 42-1467 and (b) Co_3O_4 nanocubes.

The morphology of the typically synthesized Co_3O_4 nanocubes was investigated by SEM, TEM and HRTEM, as shown in Figure 2. Clearly, the as-obtained samples consist of uniform and well-shaped cube structures with the width of several ten nanometers to several hundred nanometers. Figure 2d shows the HRTEM image of the area marked by white frame in Figure 2c, and the inset of Figure 2d is the corresponding Fast Fourier Transform (FFT) pattern. The lattice fringe can be observed clearly, and the interplane distances of adjacent lattice fringes is about 0.26 nm (2.6Å),

which is in good agreement with the *d* value of (031) plane of cubic single Co_3O_4 crystal. Besides, the sharp diffraction spots of the corresponding FFT pattern reveal the well crystalline nature of the synthesized Co_3O_4 nanocubes. Based on the above analysis, it confirms that well shaped structures and well crystalline nature of Co_3O_4 nanocubes could be synthesized via the simple hydrothermal method.

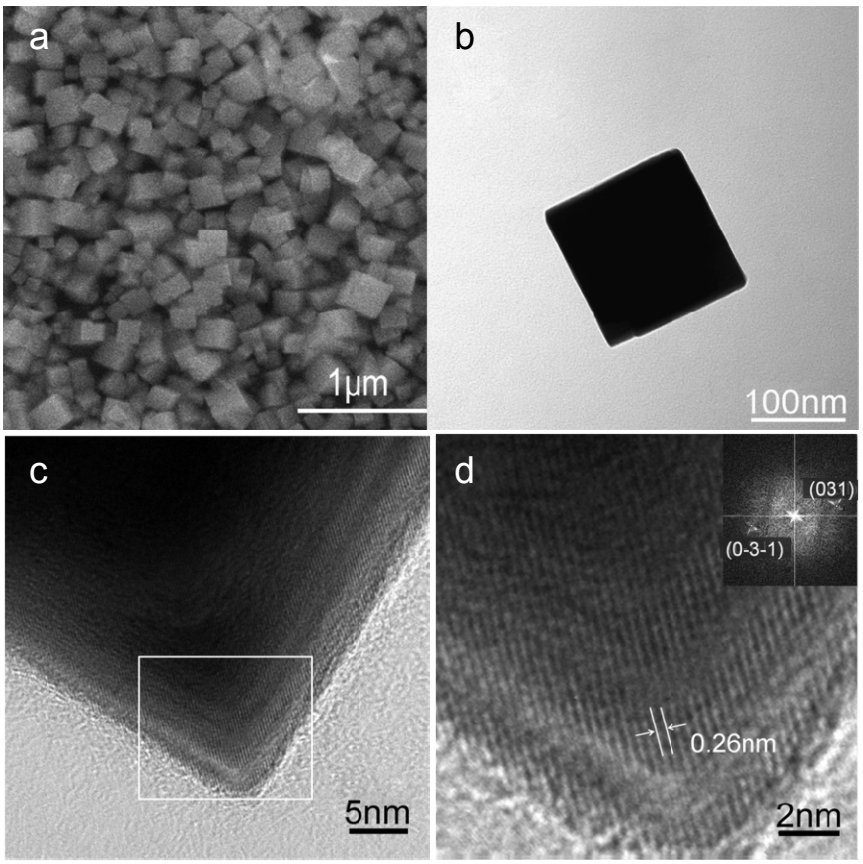

Figure 2. SEM, TEM and HRTEM images of the as-prepared Co_3O_4 nanocubes: (a) SEM, (b) TEM, (c) HRTEM, (d) enlarged image of the area marked by white frame in (c) and the corresponding FFT pattern.

3.2. Effect of synthesis conditions

To further confirm the growth mechanism, it is important to obtain more information about the formation process of the Co_3O_4 nanocubes. The effect of experiment parameters, including reaction temperature, the mole ratio of PVP to Co^{2+}, and reaction time were investigated in details.

As for the hydrothermal system, reaction temperature strongly affects the morphology of final products [25]. Firstly, contrast experiments were carried out to investigate the influence of reaction temperature on the morphology of the as-obtained Co_3O_4 samples. These experiments were carried out by only varying the reaction temperature, and 2 mM of NaSCN, 2 mM of $Co(CH_3COO)_2 \cdot 4H_2O$ and 0.003 mM PVP were used throughout the experiment. The corresponding SEM images are shown in Figure 3. The SEM result demonstrates that all of the samples obtained under different reaction temperatures contain cube-like structures; while uniform and well-shaped cube structures could be obtained only when the reaction temperature is 120 °C (Figure 3a). With the increasing of

reaction temperature, the content of irregular structures with a high degree of aggregation increases, while the percentage of cube-like structures decreases (Figure 3b–d).

In the present synthesis system, cobalt ions should exist in the form of $[Co(SCN)_x]^{2-x}$ ($0 \leqslant x \leqslant 6$), and some uncombined Co^{2+} could also exist in the solution due to the molar ratio of SCN^- to Co^{2+} is about 1. Under hydrothermal condition, $[Co(SCN)_x]^{2-x}$ could release $[Co(OH)_4]^{2-}$ via hydrolytic reactions for the formation of Co_3O_4 nucleus and its growth [6]. At relative low temperature, 120 °C, the hydrolytic reactions of $[Co(SCN)_x]^{2-x}$ could produce $[Co(OH)_4]^{2-}$ gradually, and thus it has enough time for the formation of Co_3O_4 nucleus and its growth. As a result, uniform and well-shaped cube crystals could be obtained. By contrast, higher reaction temperature would accelerate the releasing of $[Co(OH)_4]^{2-}$ as well as the growth rate of Co_3O_4 nucleus, which would make it difficult to control the growth process of Co_3O_4 nucleus. And thus, the content of cube-like structures decreases gradually, while the percentage of irregular structures and even aggregates increase with the increasing of temperature from 140 °C to 180 °C. Consequently, appropriate reaction temperature is required in order to obtain uniform and discrete Co_3O_4 nanocubes, that is, the chosen reaction temperature is 120 °C.

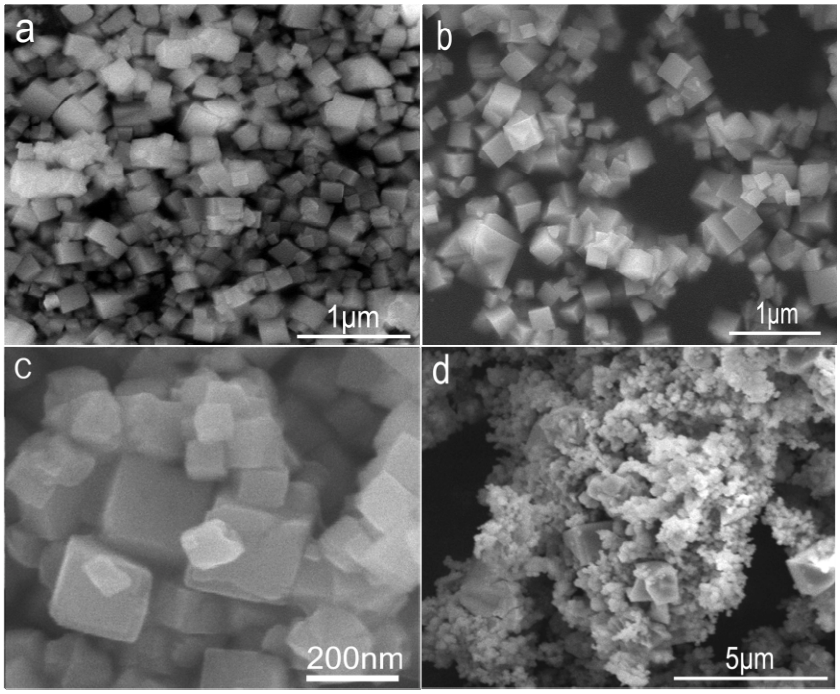

Figure 3. SEM images of samples obtained at reaction temperatures of (a) 120 °C, (b) 140 °C, (c) 160 °C and (d) 180 °C.

The amount of dispersant also has important effect on the morphology of the final products [26–28], and then several contrastive experiments were carried out to determine the role of PVP during the formation process of the Co_3O_4 nanocubes. The experiments were conducted by varying the amount of PVP added into the reaction system and maintaining the other experiment procedure and reaction conditions the same as the typical experiment. The corresponding SEM images of the obtained samples are shown in Figure 4.

It can be observed that carambola-like structures assembled by nanopetals and some cube-like structures are obtained without the presence of PVP (Figure 4a). When the mole ratio of PVP to Co^{2+}

is 0.002 and/or 0.003, cube-like structures with some irregular particles appear, and the percentage of the cube-like architectures increases with the increasing of PVP (Figure 4a–4c). This might due to PVP could disperse Co_3O_4 nucleus and prevent their agglomration during the growth process, which can inhibit the formation of irregular particles. However, when the mole ratio of PVP to Co^{2+} is higher than 0.005, only irregular particles are obtained (Figure 4d). This may be originated from the formation of PVP micelle under high concentration of PVP, and thus PVP has less effect on dispersing Co_3O_4 nucleus. The above analysis shows that proper amount of PVP could disperse Co_3O_4 nucleus effectively, leading to the formation of uniform and monodisperse cube-like structures; however, some adverse process may occur under excess amount of PVP. And the appropriate mole ratio of PVP to Co^{2+} is between 0.002 and 0.003.

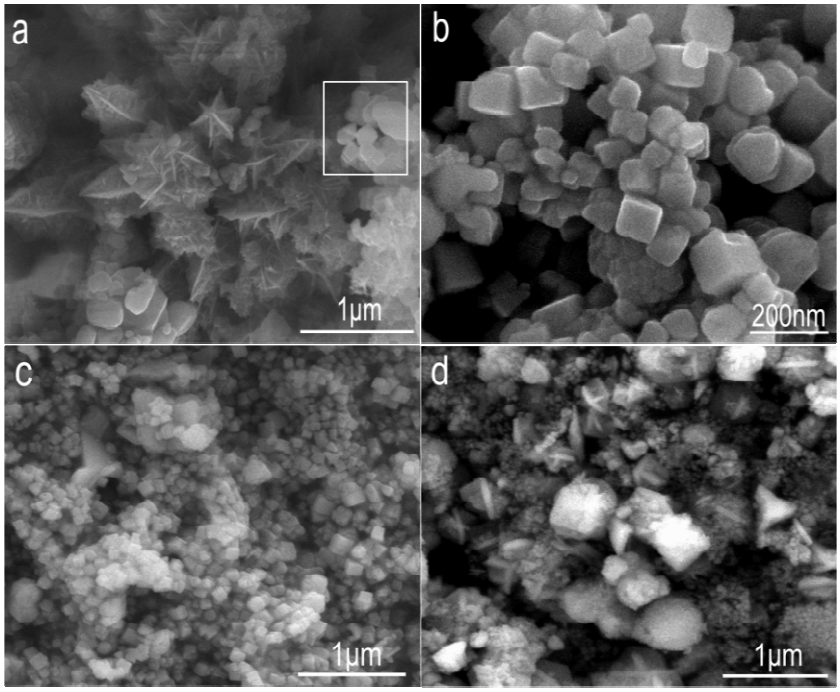

Figure 4. SEM images of samples obtained at different mole ratio of PVP to Co^{2+}: (a) 0, (b) 0.002, (c) 0.003 and (d) 0.005.

A systematic time-dependent experiment was also conducted to track the formation process of the Co_3O_4 nanocubes and investigate the growth mechanism of the cube-like Co_3O_4 structures. The synthetic time was 2, 9, 18, 27 and 36 h, respectively. The SEM results of the samples obtained at different reaction time are shown in Figure 5. It can be seen that irregular particles are obtained at the reaction time of 2 h; meanwhile, many small cube-like structures could also be observed on the surface of the irregular particles, as shown in the enlarged image of Figure 5a. Aggregates composed by cube-like structures with wide size distributions are obtained at the reaction time of 9 h (Figure 5b). When the reaction time is prolonged to 18 h, 27 h and/or 36 h, the percentage of cube-like structures with uniform size distribution increases; meanwhile, irregular particles decrease and finally disappear (Figure 5c, 5d and 2a). The corresponding XRD patterns are shown in Figure 6, which indicate that all the products are phase-pure cubic Co_3O_4 crystals. Furthermore, it can be observed that with the prolongation of reaction time, the intensity of diffraction peaks become much

stronger suggesting the improved crystallinity of the products, which is somewhat in accordance with the SEM results. As a result, the above results reveal that the reaction time is also a crucial factor for the preparation of uniform Co_3O_4 nanocubes.

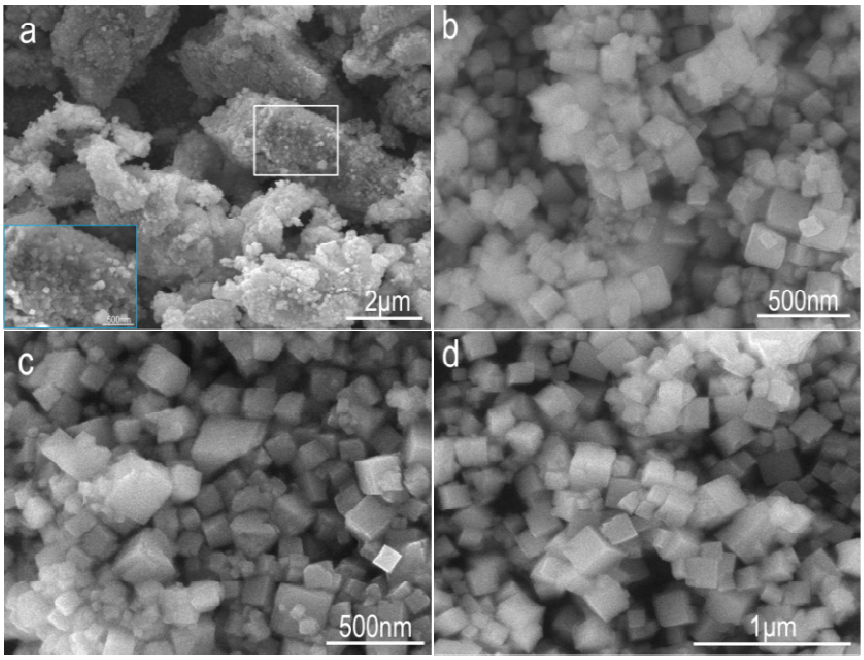

Figure 5. SEM images of samples obtained at the reaction time of (a) 2 h, (b) 9 h, (c) 18 h and (d) 27 h.

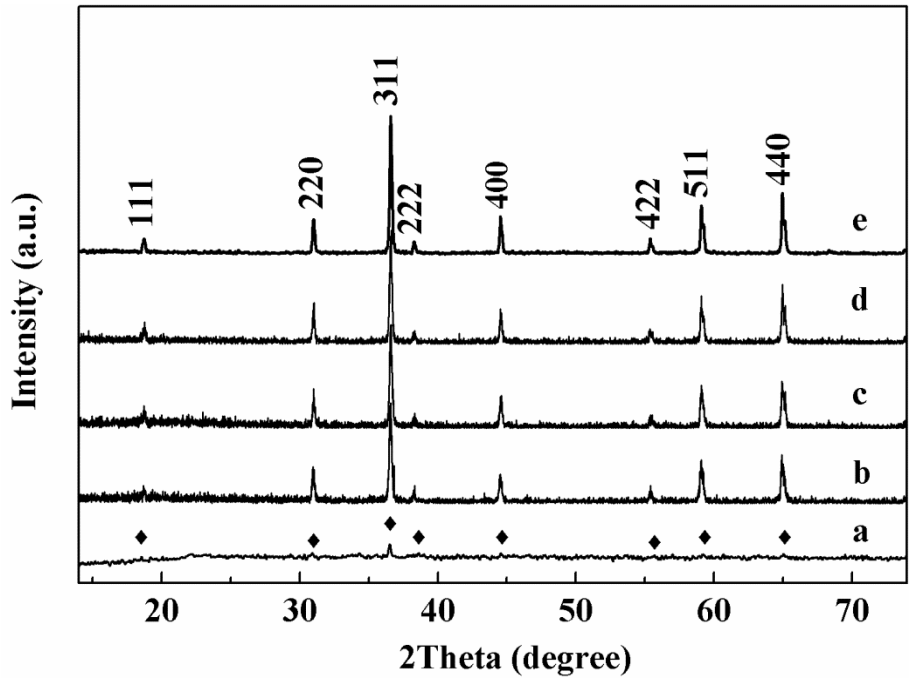

Figure 6. XRD patterns of samples obtained at the reaction time of (a) 2 h, (b) 9 h, (c) 18 h, (d) 27 h and (e) 36 h.

3.3. Possible growth mechanism of the Co_3O_4 nanocubes

On the basis of characterization results of the samples obtained under different condition-dependent experiments, a possible aggregate-dissolution-recrystallization growth mechanism is proposed to explain the formation process of the as-prepared Co_3O_4 nanocubes.

As for the present synthetic system using $Co(CH_3COO)_2 \cdot 4H_2O$ as the source of cobalt element, Co^{2+} would transform into $[Co(OH)_4]^{2-}$ and $[Co(OH)_6]^{3-}$ step by step according to the following hydrolytic reactions during the hydrothermal synthesis process.

$$Co^{2+} + xSCN^- \rightarrow [Co(SCN)_x]^{2-x} \quad (1)$$

$$CH_3COO^- + H_2O \rightarrow CH_3COOH + OH^- \quad (2)$$

$$[Co(SCN)_x]^{2-x} + nOH^- \rightarrow [Co(OH)_n]^{2-n} + xSCN^- \quad (3)$$

$$4[Co(OH)_n]^{2-n} + O_2 + 2H_2O \rightarrow 4[Co(OH)_n]^{3-n} + 4OH^- \quad (4)$$

The main form of cobalt ions would be $[Co(OH)_4]^{2-}$ in the initial hydrothermal process, and a small amount of $[Co(OH)_4]^{2-}$ would be oxidized to $[Co(OH)_6]^{3-}$ by O_2 existed in the system (reaction (4)). Undoubtedly, the cobaltous hydroxides would gather together to reduce the surface energy and thus bulky aggregates appear (Figure 5a).

On the basis of growth units' model [29], the coordination polyhedron of anions (including some cations) with similar symmetry to the unit cell could form the steadiest crystal. Consequently, Co_3O_4 atomic group would appear via the dehydration condensation reaction between the coordination polyhedron growth units of $[Co(OH)_4]^{2-}$ and $[Co(OH)_6]^{3-}$ forming the short range order structure during the following reaction process, which would consume a lot of cobalt ions. However, due to the hydrolytic process and $[Co(SCN)_x]^{2-x}$ cannot produce enough $[Co(OH)_4]^{2-}$ timely (reaction (3)), cobalt ions in the reaction system could not meet the requirement of forming Co_3O_4 atomic group. As a result, the pre-formed aggregates would dissolve and release cobalt ions to meet the needs of forming Co_3O_4 atomic group. This could be confirmed by the samples obtained at the reaction time of 2 h, which possess poor crystallinity (Figure 5a and Figure 6a). After that the previously formed Co_3O_4 atomic group would transform into crystal nuclei when the distance between the atomic groups reaches and/or exceeds the critical distance [30].

The crystallographic structure of Co_3O_4 is generally affected by the competitive growth of (111) and (100) facets, due to their higher stability in comparison with other facets. The preferred growth of (100) facet results in the formation of octahedra, whereas the preferred growth of (111) facet leads to the formation of cubes [31]. In general, the growth rate of (111) is faster than that of (100) facet, thus Co_3O_4 nanocubes are generally obtained, without the presence of any ligand. However, cube-like structures are prepared in the presence of ligand in our experiment. It might due to the fact that SCN^- possesses linear structure with no obvious steric hindrance, which could hardly restrict the other growth units diffuse to the surface of Co_3O_4 crystal nuclei. As a result, Co_3O_4 could grow in the similar way as that in the absence of any ligand, and thus cube-like structures are obtained.

Even though SCN^- has no obvious steric hindrance, it could control the growth rate of Co_3O_4 nuclei by controlling the releasing of cobalt ions from $[Co(SCN)_x]^{2-x}$. Under high temperatures (> 120 °C), the rapid hydrolytic reaction of $[Co(SCN)_x]^{2-x}$ leads to a large amount of $[Co(OH)_4]^{2-}$, which then undergoes rapid dehydration condensation under the high temperatures leading to the growth of the Co_3O_4 crystal nuclei uncontrollable (Figure 3b–d). By contrast, under proper temperature, 120 °C,

proper amount of $[Co(OH)_4]^{2-}$ is produced and the growth rate of nuclei is relative slow, so as to control the morphology and size of the final products (Figure 3a). Consequently, uniform, monodisperse and high crystallinity Co_3O_4 nanocubes are prepared.

As it can be seen from Figure 5b–d, cube-like structures are obtained at the reaction time of 9 h, 18 h and 27 h. This indicates that the morphology of Co_3O_4 would not change after the formation of the cube-like structures, and growth units containing cobalt element could absorb on the surface of the small cube-like structures leading to the growth of the cube-like crystal size in the following hydrothermal treatment. As a result, Co_3O_4 nanocubes are prepared via the growth of the cube-like Co_3O_4 crystal nuclei.

3.4. Ammonium perchlorate decomposition activity of the Co_3O_4 nanocubes

The Co_3O_4 nanocubes were explored as an additive to the thermal decomposition of AP, the key component of composite solid propellants. The catalytic property was investigated by thermal decomposition of AP, and the thermal gravimetric analysis (TGA) was carried out under N_2 atmosphere (at a flow rate of 20 mL/min) with a heating rate of 5 °C/min. The sample was prepared by blending 0.02 g Co_3O_4 with 0.98 g pure AP thoroughly, and then the mixture was dried in air at 80 °C for 6 h. For comparison, Co_3O_4 microparticles with irregular shape prepared via conventional co-precipitation method were also tested in the similar way, the results are shown in Figure 7.

The TGA curve of pure AP exhibits two weight loss steps, while only one weight loss step could be observed under the effect of Co_3O_4, which is in accordance with the previous reports [32]. The starting thermal decomposition temperatures of AP catalyzed by Co_3O_4 nanocubes and microparticles are about 254 °C and 248 °C, respectively, while the starting thermal decomposition temperature of pure AP is about 275 °C. And the final decomposition temperatures of the three samples are about 302 °C, 323 °C and 445 °C, respectively. The reported initial and final thermal decomposition temperatures for nanoflake, flower-like, multilayer stacked, nanosheet and core-shell Co_3O_4 paritcles were 273 °C, 241.1 °C, 242.2 °C, 234.7 °C, 260 °C and 342°C, 324.5 °C, 325.6 °C, 319.2 °C, 380 °C, respectively [27,28]. Clearly, the addition of 2 wt% Co_3O_4 nanocubes could decrease the decomposition temperature of AP more effectively, as compared to Co_3O_4 microparticles and the pure AP case. It was reported that AP decomposition involved two crucial steps: (1) ammonia oxidation and (2) dissociation of ClO_4^- species into ClO_3^- and O_2, and Co_3O_4 could have some effect during the two steps [33]. As a result, we propose that the relative high catalytic activity of Co_3O_4 nanocubes is probably due to the small particle size and more importantly the special exposed facets, which could provide more active sites to accelerate the two steps [6].

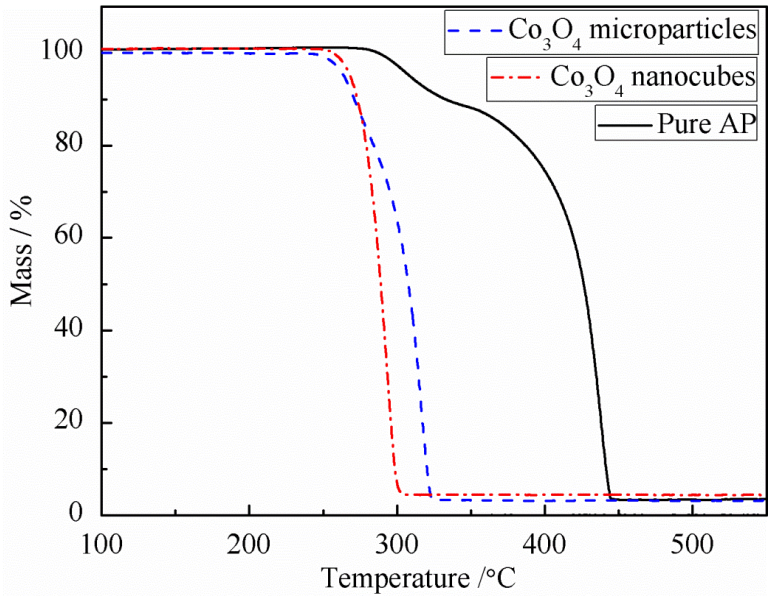

Figure 7. TG curves of the mixture of AP and Co_3O_4 nanocubes, the mixture of AP and Co_3O_4 microparticles, and pure AP.

4. Conclusions

In summary, uniform and monodisperse Co_3O_4 nanocubes were successfully synthesized by a simple hydrothermal method. The influence of reaction temperature and the amount of dispersant on the size and morphology of the as-obtained Co_3O_4 nanocubes were investigated. Based on the condition-dependent experiments, a possible aggregate-dissolution-recrystallization growth mechanism was proposed to explain the formation process of the Co_3O_4 nanocubes. The Co_3O_4 nanocubes showed noticeable promotion of AP decomposition due to the special facets crystallographic orientation of the nanocrystals. This simple method could effectively control the growth process of Co_3O_4 nanocubes, which has the potential of to be used for the controlled synthesis of some other crystals.

Acknowledgments

We are grateful to the financial supports from Doctor Foundation of Zunyi Normal College (no. BS[2014]09 and BS[2014]10).

Conflict of Interest

All authors declare no conflict of interest in this paper.

References

1. Mou XL, Zhang BS, Li Y, et al. (2012) Rod-Shaped Fe_2O_3 as an Efficient Catalyst for the Selective Reduction of Nitrogen Oxide by Ammonia. *Angew Chem Int Ed* 51: 2989–2993.

2. Muir JMR, Idriss H (2009) Formamide reactions on rutile TiO_2(011) surface. *Surf Sci* 603: 2986–2990.
3. Smith WL, Hobson AD (1973) The structure of cobalt oxide, Co_3O_4. *Acta Cryst B* 29: 362–363.
4. Petitto SC, Marsh EM, Carson GA, et al. (2008) Cobalt oxide surface chemistry: The interaction of CoO(100), Co_3O_4(110) and Co_3O_4(111) with oxygen and water. *J Mol Catal A: Chem* 281: 49–58.
5. Jang YI, Wang HF, Chiang YM (1998) Room-temperature synthesis of monodisperse mixed spinel $(Co_xMn_{1-x})_3O_4$ powder by a coprecipitation method. *J Mater Chem* 41: 2761–2764.
6. Zhou H, Lv BL, Wu D, et al. (2013) Synthesis and properties of octahedral Co_3O_4 single crystalline nanoparticles enclosed by (111) facets. *CrystEngComm* 15: 8337–8344.
7. Wang HT, Zhang L, Tan XH, et al. (2011) Supercapacitive Properties of Hydrothermally Synthesized Co_3O_4 Nanostructures. *J Phys Chem C* 115: 17599–17605.
8. Xiao XL, Liu XF, Zhao H, et al. (2012) Facile Shape Control of Co_3O_4 and the Effect of the Crystal Plane on Electrochemical Performance. *Adv Mater* 24: 5762–5766.
9. Li WY, Xu LN, Chen J (2005) Co_3O_4 Nanomaterials in Lithium-Ion Batteries and Gas Sensors. *Adv Funct Mater* 15: 851–857.
10. Jansson J, Palmqvist AEC, Fridell E, et al. (2002) On the Catalytic Activity of Co_3O_4 in Low-Temperature CO Oxidation. *J Catal* 211: 387–397.
11. Fujita S, Suzuki K, Mori T (2003) Preparation of High-Performance Co_3O_4 Catalyst for Hydrocarbon Combustion from Co-Containing Hydrogarnet. *Catal Lett* 86: 139–144.
12. Xu R, Zeng HC (2003) Mechanistic Investigation on Self-redox Decompositions of Cobalt-Hydroxide-Nitrate Compounds with Different Nitrate Anion Configurations in Interlayer Space. *Chem Mater* 15: 2040–2048.
13. Li L, Ren JC (2006) Rapid preparation of spinel Co_3O_4 nanocrystals in aqueous phase by microwave irradiation. *Mater Res Bull* 41: 2286–2290.
14. Fan YQ, Shao HB, Wang JM, et al. (2011) Synthesis of foam-like freestanding Co_3O_4 nanosheets with enhanced electrochemical activities. *Chem Commun* 47: 3469–3471.
15. Shen XP, Miao HJ, Zhao H, et al. (2008) Synthesis, characterization and magnetic properties of Co_3O_4 nanotubes. *Appl Phys A* 91: 47–51.
16. Chen Y, Zhang Y, Fu S (2007) Synthesis and characterization of Co_3O_4 hollow spheres. *Mater Lett* 61: 701–705.
17. Liu QK, Wang GH, Xu CK, et al. (2002) Fabrication of Co_3O_4 nanorods by calcination of precursor powders prepared in a novel inverse microemulsion. *Chem Commun* 14: 1486–1487.
18. Yang LX, Zhu YJ, Li L, et al. (2006) A Facile Hydrothermal Route to Flower-Like Cobalt Hydroxide and Oxide. *Eur J Inorg Chem* 2006: 4787–4792.
19. He T, Chen DR, Jiao XL, et al. (2006) Co_3O_4 Nanoboxes: Surfactant-Templated Fabrication and Microstructure Characterization. *Adv Mater* 18: 1078–1082.
20. Hu LH, Sun KQ, Peng Q, et al. (2010) Surface active sites on Co_3O_4 nanobelt and nanocube model catalysts for CO oxidation. *Nano Res* 3: 363–368.
21. Liu XH, Qiu GZ, Li XG (2005) Shape-controlled synthesis and properties of uniform spinel cobalt oxide nanocubes. *Nanotechnology* 16: 3035–3040.
22. Song XC, Wang X, Zheng YF, et al. (2011) Synthesis and electrocatalytic activities of Co_3O_4 nanocubes. *J Nanopart Res* 13: 1319–1324.

23. Lou XW, Deng D, Lee JY, et al. (2008) Self-Supported Formation of Needlelike Co_3O_4 Nanotubes and Their Application as Lithium-Ion Battery Electrodes. *Adv Mater* 20: 258–262.
24. Feng SQ, Zheng MB, Li NW, et al. (2009) Synthesis of Ordered Macroporous Co_3O_4 Microspheres via an Easy Melt Infiltration Route. *Chem Lett* 38: 1050–1051.
25. Wang L, Zhao Y, Lai QY, et al. (2010) Preparation of 3D rose-like NiO complex structure and its electrochemical property. *J Alloys Compd* 495: 82–87.
26. Rana RK, Zhang LZ, Yu JC, et al. (2003) Mesoporous Structures from Supramolecular Assembly of in situ Generated ZnS Nanoparticles. *Langmuir* 19: 5904–5911.
27. Li YC, Li XH, Yang CH, et al. (2003) Controlled synthesis of CdS nanorods and hexagonal nanocrystals. *J Mater Chem* 13: 2641–2648.
28. Yu JH, Joo J, Park HM, et al. (2005) Synthesis of Quantum-Sized Cubic ZnS Nanorods by the Oriented Attachment Mechanism. *J Am Chem Soc* 127: 5662–5670.
29. Shi EW, Chen ZZ, R. L. Yuan RL, et al. (2004) Thermal Crystallography. Beijing: Science Press.
30. Zhang L, Yu XW, Wu HP, et al. (2009) High-pressure hydrothermal synthesis and growth mechanism of Co_3O_4 nanoparticles. *Mater Eng Powder Metall* 4: 306–309.
31. Wang XX, Lv GL, Zeng YW, et al. (2003) Studies on the Nanocrystalline Co_3O_4 by Wet Synthesis and Its Microstructure. *Acta Chim. Sinica* 61: 1849–1853.
32. Jin LN, Liu Q, Sun WY (2012) Shape-controlled synthesis of Co_3O_4 nanostructures derived from coordination polymer precursors and their application to the thermal decomposition of ammonium perchlorate. *CrystEngComm* 14: 7721–7726.
33. Guan XF, Li GS, Zhou LH, et al. (2009) Template-free Approach to Core–Shell-structured Co_3O_4 Microspheres. *Chem Lett* 38: 280–281.